

Absence of room temperature ferromagnetism in bulk Mn-doped ZnO

S. Kolesnik* and B. Dabrowski

Department of Physics, Northern Illinois University, DeKalb, IL 60115

(Dated: November 3, 2021)

Structural and magnetic properties have been studied for polycrystalline $\text{Zn}_{1-x}\text{Mn}_x\text{O}$ ($x = 0.02, 0.03, 0.05$). Low-temperature ($\sim 500^\circ\text{C}$) synthesis leaves unreacted starting ZnO and manganese oxides. Contrary to a recent report, no bulk ferromagnetism was observed for single-phase materials synthesized in air at temperatures above 900°C . Single-phase samples show paramagnetic Curie-Weiss behavior.

In order to exploit spins as information carriers in functional spintronics it is necessary to develop new materials that would exhibit both room temperature ferromagnetism and semiconducting properties. Recent theoretical predictions of room temperature ferromagnetism in $\text{Zn}_{1-x}\text{M}_x\text{O}$, where $M = \text{Mn}$ (p -type),¹ or Fe, Co, Ni² motivated the study of this class of materials. In our recent paper³, we have shown that the ferromagnetic contribution to the magnetization in polycrystalline $\text{Zn}_{1-x}\text{M}_x\text{O}$ can originate from ferromagnetic impurities. A recent article in *Nature Materials* by Sharma *et al.*⁴ reported on observation of ferromagnetism above room temperature in bulk polycrystalline material and thin films of $\text{Zn}_{0.98}\text{Mn}_{0.02}\text{O}$. Sharma *et al.* claim that such materials are obtained homogeneous and uniform from the low-temperature (500 - 700°C) ceramic processing. Several papers alternatively reported the presence^{5,6,7,8,9,10,11,12} or absence^{13,14,15,16,17,18,19} of high temperature ferromagnetic ordering in $\text{Zn}_{1-x}\text{M}_x\text{O}$, which is a result of different preparation methods. Here we show that single-phase $\text{Zn}_{1-x}\text{Mn}_x\text{O}$ ($x \leq 0.05$) can be synthesized in air only at higher temperatures ($> 900^\circ\text{C}$). Low-temperature synthesis leads to incompletely reacted mixture of diamagnetic ZnO and magnetic manganese oxides. Single-phase polycrystalline $\text{Zn}_{1-x}\text{Mn}_x\text{O}$ is paramagnetic similar to other Mn-containing diluted magnetic semiconductors.

The $\text{Zn}_{1-x}\text{Mn}_x\text{O}$ ($x \leq 0.05$) samples in this study were prepared using a standard solid-state reaction, similar to that used by Sharma *et al.*⁴ Mixtures of ZnO and MnO_2 , (purity 99.999%, Johnson Matthey Materials, UK and Alfa Aesar, USA, respectively) were fired in air at 400°C for 12 hours, pressed into pellet and annealed at increasing temperatures (T_{ann}) up to 1350°C . For the high-temperature ($T_{\text{ann}} > 900^\circ\text{C}$) annealing, when Mn starts to substitute for Zn in the material, the samples were reground and re-pressed before each firing.

Magnetic ac susceptibility and dc magnetization were measured using a Physical Property Measurement System and a Magnetic Property Measurement System (both Quantum Design) at temperatures up to 400 K. X-ray diffraction (XRD) experiments have been performed using a Rigaku x-ray diffractometer. Energy dispersive x-ray spectroscopy (EDXS) analysis was performed by

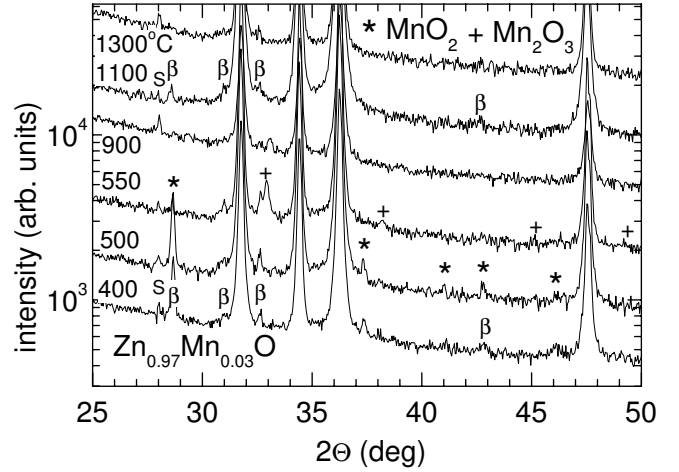


FIG. 1: Semi-logarithmic plots of x-ray diffraction (XRD) patterns for $\text{Zn}_{0.97}\text{Mn}_{0.03}\text{O}$ annealed at various temperatures (listed in the Figure). The spectra are shifted for clarity. $\text{CuK}\beta$ radiation peaks of ZnO are marked with β . Stars and crosses denote impurity peaks of MnO_2 and Mn_2O_3 , respectively. The silica standard peak is marked with 'S'.

a Hitachi S-4700-II scanning electron microscope. Thermogravimetric analysis was done with a Cahn thermobalance.

In Fig. 1, we show a semi-logarithmic plot of XRD patterns for $\text{Zn}_{0.97}\text{Mn}_{0.03}\text{O}$ annealed at various temperatures T_{ann} . Essentially, the same results were obtained for $\text{Zn}_{0.98}\text{Mn}_{0.02}\text{O}$. In all the XRD spectra, we observe the main peaks of the wurtzite structure of ZnO. Each strong peak is accompanied by a smaller peak due to incompletely filtered $\text{CuK}\beta$ radiation. Besides these peaks, secondary peaks of manganese oxides are observed after annealing at low temperatures. For $T_{\text{ann}} < 500^\circ\text{C}$, peaks of MnO_2 are observed. For $T_{\text{ann}} > 500^\circ\text{C}$, the peaks of Mn_2O_3 are visible. The transformation of the secondary phase MnO_2 to Mn_2O_3 in air is consistent with the structural transition of pure MnO_2 , observed with XRD and thermogravimetric measurements. At $T_{\text{ann}} = 500^\circ\text{C}$, both manganese oxides are present for $\text{Zn}_{1-x}\text{Mn}_x\text{O}$ samples annealed for 12 hours. The presence of manganese oxide peaks is an indication that the polycrystalline $\text{Zn}_{1-x}\text{Mn}_x\text{O}$ is not single-phase after low-temperature annealing, contrary of the conclusion drawn by Sharma *et al.* When a standard ceramic synthesis

*Electronic mail: kolesnik@physics.niu.edu

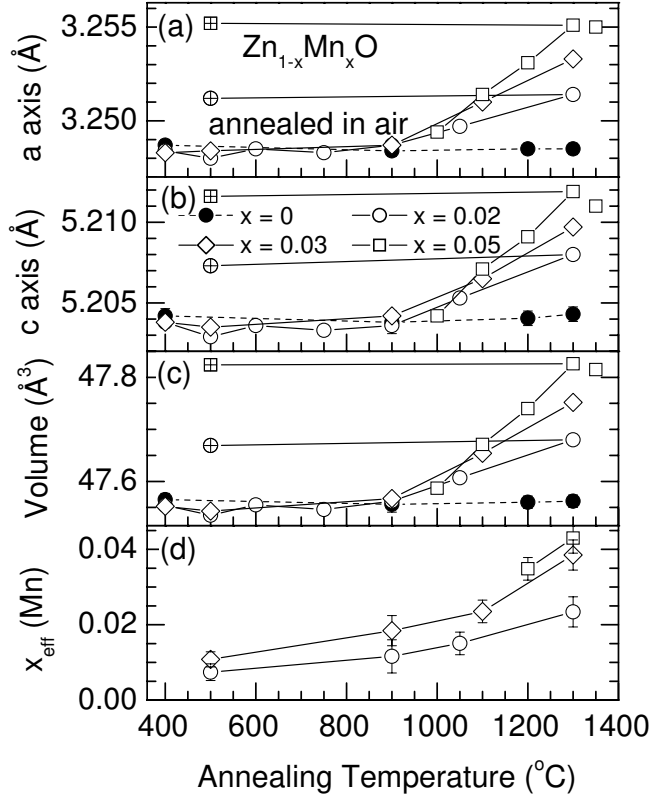


FIG. 2: (a-c) Lattice parameters for $Zn_{1-x}Mn_xO$ annealed in air at various temperatures, (d) The effective Mn content determined from the EDXS. Open symbols: substituted samples, filled circles: pure ZnO, crossed symbols: single-phase samples annealed at 500°C.

method is used, the $Zn_{1-x}Mn_xO$ compound starts to form a single-phase compound at temperatures higher than 900°C.

The Mn substitution in $Zn_{1-x}Mn_xO$ can also be easily verified by observing the change of the lattice parameters as a function of T_{ann} .³ The lattice parameters of the wurtzite structure are shown in Figs. 2(a-c), for several nominal Mn contents x . For comparison, the lattice parameters of similarly annealed pure ZnO are also shown. Fig. 2 demonstrates that the lattice parameters of $Zn_{1-x}Mn_xO$ are fairly constant and almost identical with those of pure ZnO for $T_{\text{ann}} \leq 900^\circ\text{C}$. For higher T_{ann} , the lattice constants gradually increase; this effect is evidence for substitution of Mn for Zn since Mn^{2+} is larger than Zn^{2+} .³ At $T_{\text{ann}} > 900^\circ\text{C}$, the compositions with $x = 0.02-0.05$ become single-phase. Subsequent annealing of the single-phase samples at 500°C does not significantly change the lattice parameters, indicating that the oxidation state of Mn incorporated to $Zn_{1-x}Mn_xO$ does not change.

In Fig. 3, we show scanning electron micrographs of $Zn_{0.97}Mn_{0.03}O$ pellets after annealing at various temperatures. We observe that the size of the grains increases with the increase of T_{ann} from less than 1 μm for $T_{\text{ann}} = 500^\circ\text{C}$ up to over 10 μm for $T_{\text{ann}} = 1300^\circ\text{C}$.

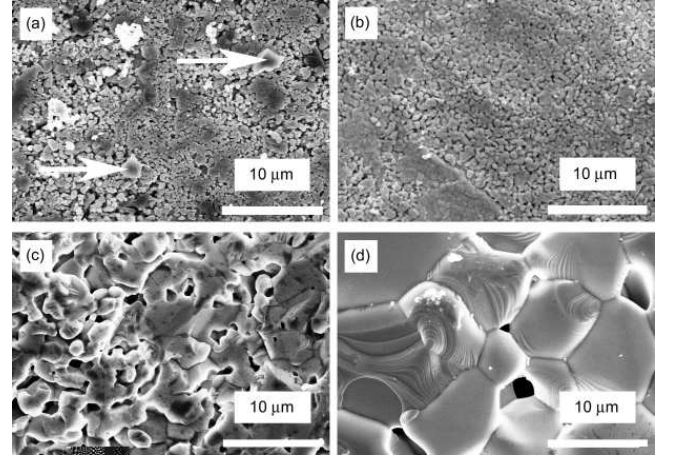


FIG. 3: Scanning electron micrographs of $Zn_{0.97}Mn_{0.03}O$ pellets after annealing in air at (a) 500°C, (b) 900°C, (c) 1100°C, and (d) 1300°C. Arrows in (a) indicate grains of pure manganese oxide.

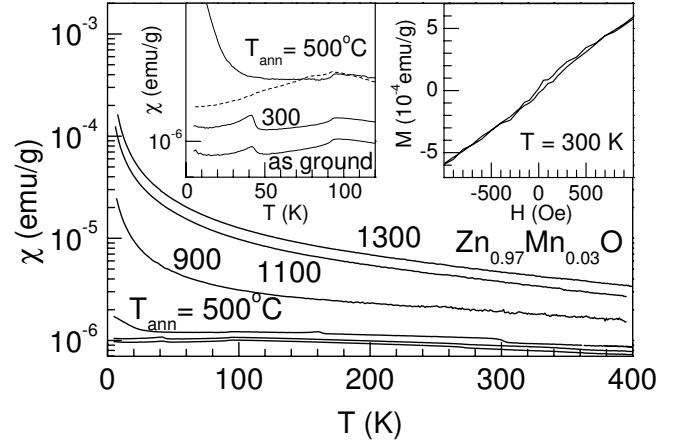


FIG. 4: Temperature dependence of the magnetic susceptibility for $Zn_{0.97}Mn_{0.03}O$ annealed at various temperatures. Left inset: low-temperature part of the main panel. Dashed line represents the magnetic susceptibility of MnO_2 annealed at 500°C, multiplied by 0.03. Right inset: the field dependence of magnetization of $Zn_{0.97}Mn_{0.03}O$ annealed at 500°C, measured at 300 K.

EDXS spectra taken on selected areas show the presence of individual grains of pure manganese oxide for $T_{\text{ann}} = 500^\circ\text{C}$ [marked with arrows in Fig. 3(a)] and pure ZnO. For higher T_{ann} , the material is more homogeneous and more substituted Mn can be detected in the grains. Fig. 2(d) presents the effective Mn content from the EDXS data. The EDXS data confirm that the Mn substitution gradually increases with increasing T_{ann} and single-phase $Zn_{1-x}Mn_xO$ ($x \leq 0.05$) forms at high temperatures ($> 900^\circ\text{C}$).

In Fig. 4, we present temperature dependencies of magnetic susceptibility for the sample with nominal composition $Zn_{0.97}Mn_{0.03}O$ annealed at various T_{ann} . The diamagnetic contribution of ZnO, equal to -0.33×10^{-6}

emu/g, was subtracted from the measured data. For $T_{\text{ann}} < 500^\circ\text{C}$, the susceptibility follows the temperature dependence expected for manganese oxides that were observed in the XRD spectra. The antiferromagnetic transition of MnO_2 can be seen at $T_N = 92$ K and in addition a very small contribution ($\sim 0.01\%$) of ferromagnetic Mn_3O_4 with $T_C = 43$ K is visible. The Mn_3O_4 present in trace amounts in the original MnO_2 (see: left inset to Fig 4) shows how apparent vestiges of ferromagnetic impurities are in susceptibility data. Note that for correct identification of such phases it is critical to perform temperature dependent measurements. For $T_{\text{ann}} = 500^\circ\text{C}$, the antiferromagnetic transition of Mn_2O_3 is also present at $T_N = 76$ K. This behavior is expected for an incompletely reacted mixture of ZnO and manganese oxides. As a reference, we have also plotted the magnetic susceptibility for MnO_2 (dashed line in the left inset to Fig. 4) annealed at 500°C , multiplied by 0.03. This curve matches well the magnetic susceptibility for $\text{Zn}_{0.97}\text{Mn}_{0.03}\text{O}$ for $T_{\text{ann}}=500^\circ\text{C}$, except for low temperatures, where a weak paramagnetic contribution is observed for $\text{Zn}_{0.97}\text{Mn}_{0.03}\text{O}$, probably due to a partial substitution of Mn for Zn in the grain boundaries region. For higher T_{ann} , when Mn is incorporated into the ZnO crystal lattice structure, the material becomes paramagnetic and the susceptibility increases one hundredfold. This reflects the random distribution of the low concentration of Mn^{2+} ions on the lattice sites and is characteristic of diluted magnetic semiconductors. No ferromagnetism at room temperature was detected for

any of the studied $\text{Zn}_{1-x}\text{Mn}_x\text{O}$ samples. Generally, the magnetization shows a linear dependence on the applied magnetic field. Occasionally, a very small hysteretic contribution to the magnetization can be observed, but it is always traced to the contamination of the sample holder (see: right inset to Fig 4).

In summary, we have synthesized polycrystalline $\text{Zn}_{1-x}\text{Mn}_x\text{O}$ ($x \leq 0.05$). This compound can be formed at temperatures higher than 900°C using a ceramic route and shows paramagnetic properties analogous to other diluted magnetic semiconductors. Low-temperature annealing leaves an incompletely reacted mixture of ZnO and manganese oxides. No bulk ferromagnetism can be observed for any of the studied samples. At the moment, the origin of the room temperature ferromagnetic behavior observed by Sharma *et al.*⁴ is not clear. Nevertheless, we provide here conclusive evidence that the samples that exhibit ferromagnetism or antiferromagnetism are not single-phase $\text{Zn}_{1-x}\text{Mn}_x\text{O}$ compounds.

Acknowledgments

This work was supported by NSF (DMR-0302617), the U.S. Department of Education, and the State of Illinois under HECA. The EDXS analysis was performed in the Electron Microscopy Center, Argonne National Laboratory, Argonne, IL.

-
- ¹ T. Dietl, H. Ohno, F. Matsukura, J. Cibert, and D. Fer-
rand, *Science* **287**, 1019 (2000).
 - ² K. Sato and H. Katayama-Yoshida, *Jpn. J. Appl. Phys.*
40, L334, (2001).
 - ³ S. Kolesnik, B. Dabrowski, and J. Mais, *J. Appl. Phys.* **95**,
2582 (2004).
 - ⁴ P. Sharma, A. Gupta, K. V. Rao, F. J. Owens, R. Sharma,
R. Ahuja, J. M. Osorio Guillen, B. Johansson, and G. A.
Gehring, *Nature Materials* **2**, 673 (2003).
 - ⁵ K. Ueda, H. Tabata, and T. Kawai, *Appl. Phys. Lett.* **79**,
988 (2001).
 - ⁶ Y. M. Cho, W. K. Choo, H. Kim, D. Kim, and Y. E. Ihm,
Appl. Phys. Lett. **80**, 3358 (2002).
 - ⁷ H.-J. Lee, S.-Y. Jeong, C. R. Cho, and C. H. Park, *Appl.*
Phys. Lett. **81**, 4020 (2002).
 - ⁸ D. P. Norton, S. J. Pearton, A. F. Hebard, N. Theodor-
opoulou, L. A. Boatner, and R. G. Wilson, *Appl. Phys.*
Lett. **82**, 239 (2003).
 - ⁹ W. Prellier, A. Fouchet, B. Mercey, Ch. Simon, and B.
Raveau, *Appl. Phys. Lett.* **82**, 3490 (2003).
 - ¹⁰ D. P. Norton, M. E. Overberg, S. J. Pearton, K. Pruessner,
J. D. Budai, L. A. Boatner, M. F. Chisholm, J. S. Lee, Z.
G. Khim, Y. D. Park, and R. G. Wilson, *Appl. Phys. Lett.*
83, 5488 (2003).
 - ¹¹ K. Ip, R. M. Frazier, Y. W. Heo, D. P. Norton, C. R. Aber-
nathy, S. J. Pearton, J. Kelly, R. Rairigh, A. F. Hebard, J.
M. Zavada, and R. G. Wilson, *J. Vac. Sci. Technol. B* **21**,
1476 (2003).
 - ¹² P. V. Radovanovic and D. R. Gamelin, *Phys. Rev. Lett.*
91, 157202 (2003).
 - ¹³ T. Fukumura, Z. Jin, M. Kawasaki, T. Shono, T.
Hasegawa, S. Koshihara, and H. Koinuma, *Appl. Phys.*
Lett. **78**, 958 (2001).
 - ¹⁴ J. H. Kim, H. Kim, D. Kim, Y. E. Ihm, and W. K. Choo,
J. Appl. Phys. **92**, 6066 (2002).
 - ¹⁵ A. Tiwari, C. Jin, A. Kvit, D. Kumar, J. F. Muth, and J.
Narayan, *Solid State Commun.* **121**, 371 (2002).
 - ¹⁶ A. S. Risbud, N. A. Spaldin, Z. Q. Chen, S. Stemmer, and
R. Seshadri, *Phys. Rev. B* **68**, 205202 (2003).
 - ¹⁷ K. Rode, A. Anane, R. Mattana, J.-P. Contour, O. Du-
rand, and R. LeBourgeois, *J. Appl. Phys.* **93**, 7676 (2003).
 - ¹⁸ X. M. Cheng and C. L. Chien, *J. Appl. Phys.* **93**, 7876
(2003).
 - ¹⁹ S. S. Kim, J. H. Moon, B.-T. Lee, O. S. Song, and J. H.
Je, *J. Appl. Phys.* **95**, 454 (2004).